Electron-Hole Asymmetry of Spin Injection and Transport in Single-Layer Graphene

Wei Han, W. H. Wang,* K. Pi, K. M. McCreary, W. Bao, Yan Li, F. Miao, C. N. Lau, and R. K. Kawakami†
Department of Physics and Astronomy, University of California, Riverside, California 92521, USA
(Received 10 December 2008; published 2 April 2009)

Spin-dependent properties of single-layer graphene (SLG) have been studied by nonlocal spin valve measurements at room temperature. Gate voltage dependence shows that the nonlocal magnetoresistance (MR) is proportional to the conductivity of the SLG, which is the predicted behavior for transparent ferromagnetic-nonmagnetic contacts. While the electron and hole bands in SLG are symmetric, gate voltage and bias dependence of the nonlocal MR reveal an electron-hole asymmetry in which the nonlocal MR is roughly independent of bias for electrons, but varies significantly with bias for holes.

DOI: 10.1103/PhysRevLett.102.137205 PACS numbers: 75.47.−m, 72.25.Hg, 73.63.−b, 85.75.−d

Graphene is an attractive material for spintronics due to its tunable carrier concentration [1–3], weak spin-orbit coupling, predictions of novel spin-dependent behavior [4,5], and the recent experimental observations of spin transport [6–12]. A special property of single-layer graphene (SLG) is that the band structure of the electrons and holes are ideally symmetric (similar to carbon nanotubes [13]), so their spin-dependent properties are expected to match. This differs from conventional semiconductors such as GaAs and Si, whose electron and hole bands are highly asymmetric (e.g., different atomic orbital states, different spin-orbit coupling, different effective masses), which leads to very different spin-dependent properties. Thus, the observation of electron-hole asymmetry of a spin-dependent property in SLG would create a unique opportunity to investigate the relationship between carrier charge and spin, separated from the typical effects of band asymmetries found in conventional semiconductors.

In this Letter, we report the observation of electron-hole asymmetry for spin injection and transport in SLG at room temperature, as determined by nonlocal magnetoresistance (MR) measurements on SLG spin vales with transparent Co contacts [14,15]. A systematic investigation of the gate voltage dependence and bias dependence of the nonlocal MR signal shows that when the carriers in the SLG are electrons, the nonlocal MR is roughly constant as a function of dc current bias, which is consistent with the standard one dimensional (1D) drift-diffusion model of spin injection and transport [15–19]. When the carriers in the SLG are holes, however, the nonlocal MR is strongly reduced in the negative bias regime (i.e., spin extraction [20]). This differing behavior between the electrons and the holes is a clear demonstration of spin-dependent electron-hole asymmetry, which is most likely due to an interfacial effect at the Co/SLG contact. Understanding the origin of this asymmetry will be crucial for the development of bipolar spin transport devices utilizing both electrons and holes.

The devices consist of exfoliated SLG sheets [21,22] and Co electrodes fabricated by electron-beam lithography using PMMA/MMA bilayer resist [Fig. 1(a)]. The SiO_2/Si substrate (300 nm layer thickness of SiO_2) is used as a gate. Because the nonlocal spin signal should be enhanced by decreasing the contact area [19], we utilize angle evaporation to deposit a 2 nm MgO masking layer prior to the deposition of an 80 nm Co layer [Fig. 1(a) detail]. This reduces the width of the contact area to ~50 nm. Prior to lift-off, the device is capped with 5 nm Al_2O_3 to protect the Co from further oxidation. For the two representative samples (*A* and *B*), the widths of the electrodes are 225, 210, 175, and 225 nm for sample *A* and 350, 160, 210, and 180 nm for sample *B*. The spacings between electrodes for

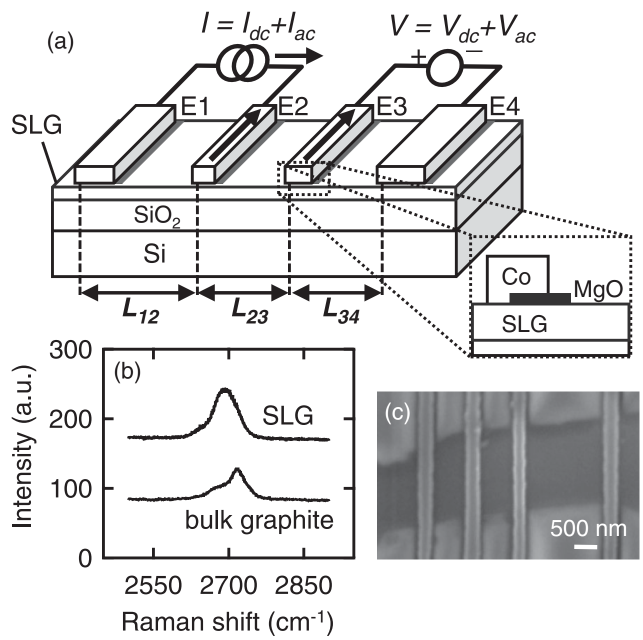

FIG. 1. (a) Schematic diagram of the single-layer graphene (SLG) spin valve. *E*1, *E*2, *E*3, are *E*4 are four cobalt electrodes. The Si substrate acts as a back gate. Detail: A MgO layer deposited by angle evaporation to reduce the width of the contact area to ~50 nm. (b) Raman spectroscopy of SLG and bulk graphite. (c) SEM image of a completed device. The darker region corresponds to the SLG.

sample A are $L_{12} = 1.0\ \mu$m, $L_{23} = 1.0\ \mu$m, and $L_{34} = 2.0\ \mu$m and for sample B are $L_{12} = 1.6\ \mu$m, $L_{23} = 1.0\ \mu$m, and $L_{34} = 1.1\ \mu$m. The widths of the SLG are $\sim 2\ \mu$m for both samples. Raman spectroscopy is used to verify the thickness of the graphene [23]. Figure 1(b) shows typical spectra from SLG measured on our devices and from bulk graphite for reference. Figure 1(c) shows a scanning electron microscope image of a completed device, in which the darker region corresponds to the SLG.

The electrical and nonlocal magnetoresistance (MR) characteristics are measured in vacuum at room temperature. Figures 2(a) and 2(b) show the resistivity of the SLG as a function of gate voltage for samples A and B. Both samples exhibit a peak in resistivity which define the Dirac point, with $V_{\mathrm{Dirac}} = -34$ V for sample A and $V_{\mathrm{Dirac}} = -32$ V for sample B. Sample A has a mobility of 900–1700 $\mathrm{cm}^2/\mathrm{V\,s}$, while sample B has a mobility of 800–1300 $\mathrm{cm}^2/\mathrm{V\,s}$. The I-V curves measured across electrodes $E1$ and $E2$ at different gate voltages indicate transparent contacts between the Co and SLG [Figs. 2(c) and 2(d)].

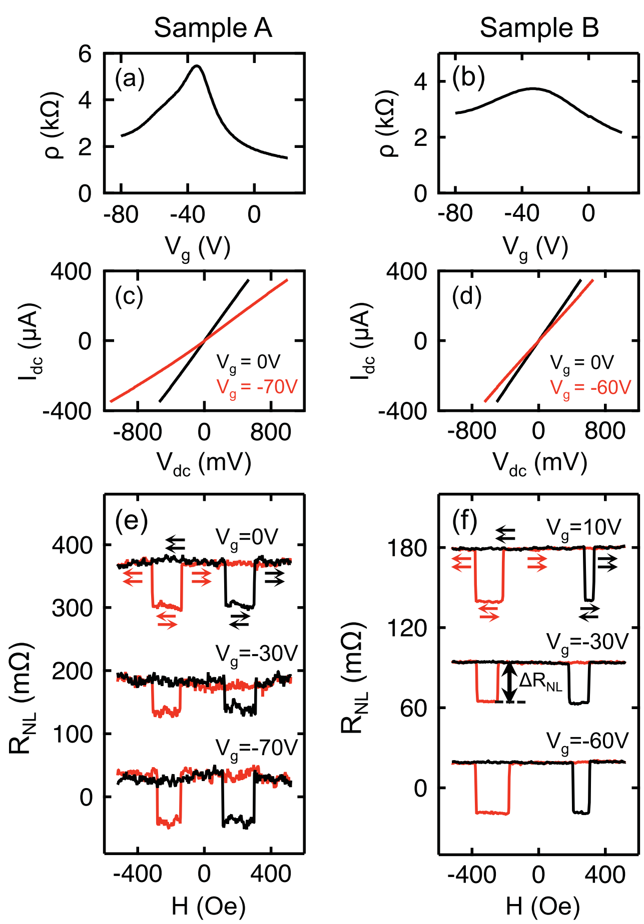

FIG. 2 (color). Electrical characteristics and nonlocal magnetoresistance (MR) scans of sample A and sample B. (a),(b) SLG resistivity vs gate voltage of sample A and sample B. (c),(d) I-V curves between electrodes $E1$ and $E2$ of sample A and sample B. (e) Nonlocal MR scans of sample A at three different gate voltages ($V_g = 0$ V, -30 V, and -70 V), as the magnetic field is swept up (black curve) and swept down (red curve). A constant background is subtracted and the curves are offset for clarity. (f) Nonlocal MR scans of sample B at $V_g = 10$ V, -30 V, and -60 V. A constant background is subtracted and the curves are offset for clarity.

Spin injection and transport are investigated using standard lock-in techniques. A current source applies a dc bias (I_{dc}) and ac excitation ($I_{\mathrm{ac}} = 30\ \mu$A) across electrodes $E1$ and $E2$ [Fig. 1(a)] to generate spin polarization in the SLG beneath electrode $E2$ by spin injection or extraction. This spin polarization propagates to $E3$ via spin diffusion and generates a nonlocal voltage across electrodes $E3$ and $E4$ ($V = V_{\mathrm{dc}} + V_{\mathrm{ac}}$) due to the spin-sensitive nature of the ferromagnetic electrodes [14–19]. To separate the spin signal from a constant background level, R_{NL} ($\equiv V_{\mathrm{ac}}/I_{\mathrm{ac}}$) is measured as the magnetic field is swept up and swept down [Figs. 2(e) and 2(f)] to generate parallel and antiparallel alignments of the central electrodes ($E2$ and $E3$). The nonlocal MR is defined as $\Delta R_{\mathrm{NL}} = R_{\mathrm{NL}}^{P} - R_{\mathrm{NL}}^{\mathrm{AP}}$, where R_{NL}^{P} ($R_{\mathrm{NL}}^{\mathrm{AP}}$) is the nonlocal resistance for the parallel (antiparallel) state. Figure 2(e) shows representative nonlocal MR scans on sample A measured at zero bias. Comparing the scans, we see that ΔR_{NL} is smallest near the Dirac point ($V_g = -30$ V) and larger for electron doping ($V_g = 0$ V) and hole doping ($V_g = -70$ V). The nonlocal MR of sample B shows similar behavior, with ΔR_{NL} smallest when V_g is close to the Dirac point, and higher for larger carrier densities [Fig. 2(f)].

Figures 3(a) and 3(b) show the detailed gate dependence of ΔR_{NL} at zero bias on samples A and B (circles). ΔR_{NL} has a minimum near the Dirac point and has increasing values for increasing electron density ($V_g > V_{\mathrm{Dirac}}$) as well as for increasing hole density ($V_g < V_{\mathrm{Dirac}}$). This behavior can be understood in terms of the 1D drift-diffusion model, which predicts that ΔR_{NL} should be proportional to the conductivity of the nonmagnetic material σ_N (SLG in our case) for transparent ferromagnetic-nonmagnetic contacts [e.g., Eq. (4) in Ref. [18], Eq. (1) in Ref. [15] with $M \gg 1$]. The solid lines in Figs. 3(a) and 3(b) show the conductivity as a function of gate voltage. The good agreement indicates that we have realized the $\Delta R_{\mathrm{NL}} \sim \sigma_N$ dependence for transparent contacts. This illustrates a powerful aspect of graphene as a material to examine spin-polarized transport, where the ability to tune the conductivity provides a novel approach to investigate theoretical predictions.

To gain insight into the characteristics of spin injection and transport in SLG, we systematically investigate the gate dependence and bias dependence of ΔR_{NL}. Figures 3(c) and 3(d) show the gate dependence of ΔR_{NL} for samples A and B for $I_{\mathrm{dc}} = +300\ \mu$A (squares), 0 μA (circles), and $-300\ \mu$A (triangles). The polarity of I_{dc} is defined in Figure 1(a). For positive bias, the gate dependence of ΔR_{NL} follows the zero bias data. On the other

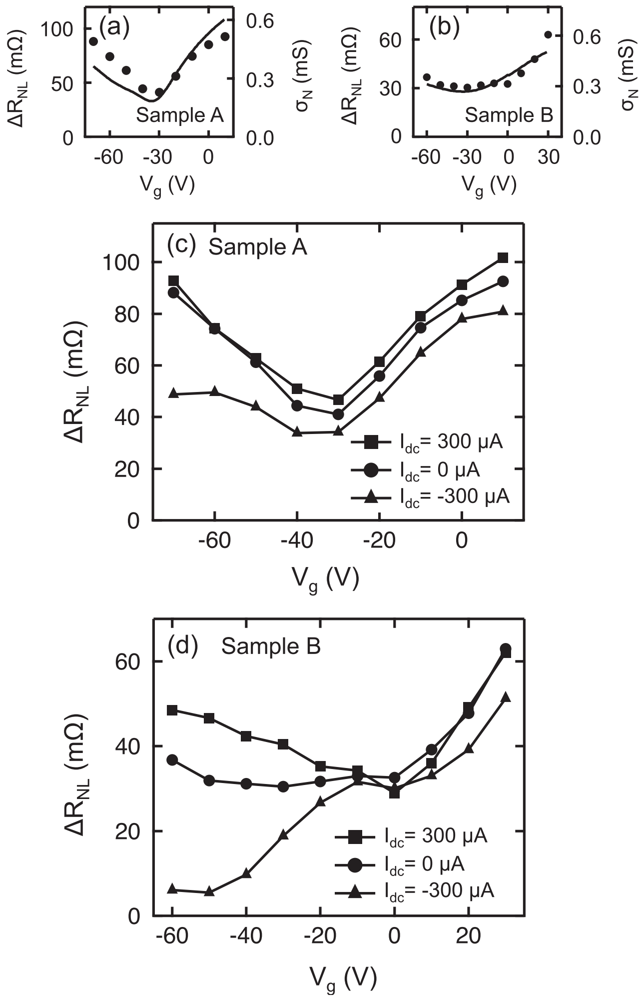

FIG. 3. (a) Nonlocal MR at zero bias (circles) and conductivity (solid line) vs gate voltage for sample A. (b) Nonlocal MR at zero bias (circles) and conductivity (solid line) vs gate voltage for sample B. (c) The dependence of nonlocal MR on the gate voltage for sample A at bias current 300 μA (squares), 0 μA (circles), -300 μA (triangles). (d) The dependence of nonlocal MR on the gate voltage for sample B at bias current 300 μA (squares), 0 μA (circles), -300 μA (triangles).

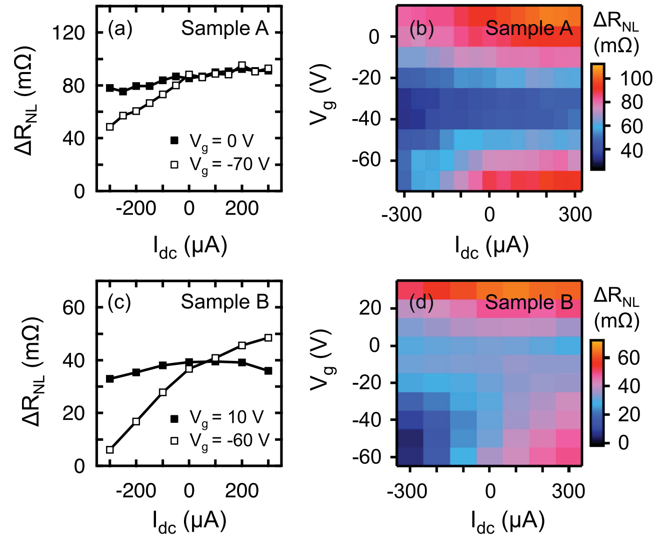

FIG. 4 (color). (a) Nonlocal MR as a function of dc bias current for sample A at $V_g = 0$ V (electrons, solid squares) and -70 V (holes, open squares). (b) Nonlocal MR as a function of gate voltage and dc bias current for sample A. (c) Nonlocal MR as a function of dc bias current for sample B at $V_g = 10$ V (electrons, solid squares) and -60 V (holes, open squares). (d) Nonlocal MR as a function of gate voltage and dc bias current for sample B.

hand, when the bias is negative and the carriers are holes (triangles, $V_g < V_{\rm Dirac}$), a strong reduction of $\Delta R_{\rm NL}$ is observed in both samples. In this case, the holes in the SLG are driven toward electrode $E2$ and become spin-polarized due to spin-dependent reflection from the ferromagnetic interface (i.e., spin extraction [20]). A very interesting aspect is that the reduction of $\Delta R_{\rm NL}$ is observed for spin extraction of holes, but not for the spin extraction of electrons.

Figure 4(a) shows the bias dependence of $\Delta R_{\rm NL}$ on sample A for $V_g = 0$ V (electrons, solid squares) and for $V_g = -70$ V (holes, open squares). For electrons, there is only a slight variation in $\Delta R_{\rm NL}$ as a function of $I_{\rm dc}$. For holes at positive bias, the behavior of $\Delta R_{\rm NL}$ is similar to the electron case. For holes at negative bias, however, there is a significantly stronger variation of $\Delta R_{\rm NL}$ as a function of dc current bias, with decreasing $\Delta R_{\rm NL}$ at larger negative biases. Figure 4(c) shows the bias dependence of $\Delta R_{\rm NL}$ on sample B for $V_g = 10$ V (electrons, solid squares) and for $V_g = -60$ V (holes, open squares). Similar to sample A, for electrons the value of $\Delta R_{\rm NL}$ is roughly constant as a function of dc bias current. For holes under negative bias, there is a very strong change of $\Delta R_{\rm NL}$ with dc current bias, nearly approaching zero at $I_{\rm dc} = -300$ μA. The images in Figs. 4(b) and 4(d) show the dependence of $\Delta R_{\rm NL}$ as a function of both gate voltage and dc current bias for samples A and B, respectively. The two main trends, namely, the roughly constant $\Delta R_{\rm NL}$ vs $I_{\rm dc}$ for electrons and the reduced $\Delta R_{\rm NL}$ for hole spin extraction, can be clearly seen in the two images.

The roughly constant $\Delta R_{\rm NL}$ vs $I_{\rm dc}$ can be understood in terms of the 1D drift-diffusion model [15–19], which predicts that the nonlocal voltage $\Delta V = \Delta V^P - \Delta V^{\rm AP}$ is proportional to the injection current I. For the ac lock-in measurement, this behavior will lead to a constant $\Delta R_{\rm NL}$ vs $I_{\rm dc}$ because the lock-in measures the slope of the ΔV vs I curve. The reduction of $\Delta R_{\rm NL}$ for hole spin extraction represents a deviation from the standard behavior. Similar deviations from the standard behavior have been observed for spin extraction in Fe/n-GaAs [24], CoFe/Al_2O_3/Al [25], and very recently in Co/Al_2O_3/graphene [26]. In these studies, tunnel barriers between the ferromagnet and nonmagnetic materials play a prominent role in explaining the unusual behavior [20,25,27]. In our devices, the contact resistances are less than 300 Ω and have linear *I-V* characteristics, so the behavior is not related to interfacial barriers and must originate from a different physical mechanism. We believe an interfacial effect at the Co/SLG contact such as wave function hybridization or local doping could be important [28–31]. With a strong Co-SLG hybridization, it is possible for the spin-dependent density of states of the Co to break the electron-hole symmetry of the SLG [30]. Apart from band structure effects, local doping has been shown to generate electron-hole asymmetry of the conductance [28,29,31], but its influence on the spin-dependent properties is currently unclear. Further theoretical and experimental studies will be needed to understand the origin of the electron-hole asymmetry of the spin signal.

In summary, we have measured nonlocal MR on SLG spin valves as a function of gate voltage and dc current bias. The gate dependence of the nonlocal MR at zero bias is found to scale with the SLG conductivity, consistent with the predicted behavior for transparent contacts. For electrons, the nonlocal MR is roughly independent of bias, but for holes under negative bias the nonlocal MR is strongly reduced. Understanding the origin of this effect should be important for further theoretical developments in spintronics.

We acknowledge the support of ONR (N00014-05-1-0568), NSF (CAREER DMR-0450037), NSF (CAREER DMR-0748910), NSF (MRSEC DMR-0820414), and CNID (ONR/DMEA-H94003-07-2-0703).

*Present address: Institute of Atomic and Molecular Sciences, Academia Sinica, Taipei 106, Taiwan.
†roland.kawakami@ucr.edu

[1] K. S. Novoselov, A. K. Geim, S. V. Morozov, D. Jiang, Y. Zhang, S. V. Dubonos, I. V. Grigorieva, and A. A. Firsov, Science **306**, 666 (2004).
[2] K. S. Novoselov, A. K. Geim, S. V. Morozov, D. Jiang, M. I. Katsnelson, I. V. Grigorieva, S. V. Dubonos, and A. A. Firsov, Nature (London) **438**, 197 (2005).
[3] Y. Zhang, Y.-W. Tan, H. L. Stormer, and P. Kim, Nature (London) **438**, 201 (2005).
[4] Y.-W. Son, M. L. Cohen, and S. G. Louie, Nature (London) **444**, 347 (2006).
[5] W. Y. Kim and K. S. Kim, Nature Nanotech. **3**, 408 (2008).
[6] E. W. Hill, A. K. Geim, K. S. Novoselov, F. Schedin, and P. Blake, IEEE Trans. Magn. **42**, 2694 (2006).
[7] N. Tombros, C. Jozsa, M. Popinciuc, H. T. Jonkman, and B. J. van Wees, Nature (London) **448**, 571 (2007).
[8] M. Ohishi, M. Shiraishi, R. Nouchi, T. Nozaki, T. Shinjo, and Y. Suzuki, Jpn. J. Appl. Phys. **46**, L605 (2007).
[9] M. Nishioka and A. M. Goldman, Appl. Phys. Lett. **90**, 252505 (2007).
[10] S. Cho, Y.-F. Chen, and M. S. Fuhrer, Appl. Phys. Lett. **91**, 123105 (2007).
[11] W. H. Wang, K. Pi, Y. Li, Y. F. Chiang, P. Wei, J. Shi, and R. K. Kawakami, Phys. Rev. B **77**, 020402(R) (2008).
[12] H. Goto, A. Kanda, T. Sato, S. Tanaka, Y. Ootuka, S. Odaka, H. Miyazaki, K. Tsukagohi, and Y. Aoyagi, Appl. Phys. Lett. **92**, 212110 (2008).
[13] P. Jarillo-Herrero, S. Sapmaz, C. Dekker, L. P. Kouwenhoven, and H. S. J. van der Zant, Nature (London) **429**, 389 (2004).
[14] M. Johnson, and R. H. Silsbee, Phys. Rev. Lett. **55**, 1790 (1985).
[15] F. J. Jedema, A. T. Filip, and B. J. van Wees, Nature (London) **410**, 345 (2001).
[16] P. C. van Son, H. van Kempen, and P. Wyder, Phys. Rev. Lett. **58**, 2271 (1987).
[17] T. Valet and A. Fert, Phys. Rev. B **48**, 7099 (1993).
[18] S. Takahashi and S. Maekawa, Phys. Rev. B **67**, 052409 (2003).
[19] T. Kimura, Y. Otani, and J. Hamrle, Phys. Rev. B **73**, 132405 (2006).
[20] H. Dery and L. J. Sham, Phys. Rev. Lett. **98**, 046602 (2007).
[21] F. Miao, S. Wijeratne, Y. Zhang, U. C. Coskun, W. Bao, and C. N. Lau, Science **317**, 1530 (2007).
[22] W. H. Wang, W. Han, K. Pi, K. M. McCreary, F. Miao, W. Bao, C. N. Lau, and R. K. Kawakami, Appl. Phys. Lett. **93**, 183107 (2008).
[23] A. C. Ferrari, J. C. Meyer, V. Scardaci, C. Casiraghi, M. Lazzeri, S. Piscanec, D. Jiang, K. S. Novoselov, S. Roth, and A. K. Geim, Phys. Rev. Lett. **97**, 187401 (2006).
[24] X. Lou, C. Adelmann, S. A. Crooker, E. S. Garlid, J. Zhang, K. S. Madhukar Reddy, S. D. Flexner, C. J. Palmstrom, and P. A. Crowell, Nature Phys. **3**, 197 (2007).
[25] S. O. Valenzuela, D. J. Monsma, C. M. Marcus, V. Narayanamurti, and M. Tinkham, Phys. Rev. Lett. **94**, 196601 (2005).
[26] C. Józsa, M. Popinciuc, N. Tombros, H. T. Jonkman, and B. J. van Wees, Phys. Rev. B **79**, 081402(R) (2009).
[27] A. N. Chantis, K. D. Belashchenko, D. L. Smith, E. Y. Tsymbal, M. van Schilfgaarde, and R. C. Albers, Phys. Rev. Lett. **99**, 196603 (2007).
[28] B. Huard, N. Stander, J. A. Sulpizio, and D. Goldhaber-Gordon, Phys. Rev. B **78**, 121402 (2008).
[29] J. Cayssol, B. Huard, and D. Goldhaber-Gordon, Phys. Rev. B **79**, 075428 (2009).
[30] G. Giovannetti, P. A. Khomyakov, G. Brocks, V. M. Karpan, J. van den Brink, and P. J. Kelly, Phys. Rev. Lett. **101**, 026803 (2008).
[31] P. Blake, R. Yang, S. V. Morozov, F. Schedin, L. A. Ponomarenko, A. A. Zhukov, I. V. Grigorieva, K. S. Novoselov, and A. K. Geim, arXiv:0811.1459.